Supplementary Materials

Sensing single molecule under micromanipulation to quantify nucleic acids

Qiang Zeng[1#], Xiaoyan Zhou[1#], Yuting Yang[2#], Jingan Wang[1], Chunhui Zhai[1], Hui Yu[1,3*]

[1]School of Biomedical Engineering, Shanghai Jiao Tong University, Shanghai, 200030, People's Republic of China

[2]Department of Instrument Science and Engineering, School of Electronic Information and Electrical Engineering, Shanghai Jiao Tong University, Shanghai, 200030, People's Republic of China

[3]Institute of Medical Robotics, Shanghai Jiao Tong University, Shanghai, 200030, People's Republic of China

[#]These authors contributed equally to this work.

[*]Correspondence should be addressed to: H.Y. (hui.yu@sjtu.edu.cn)

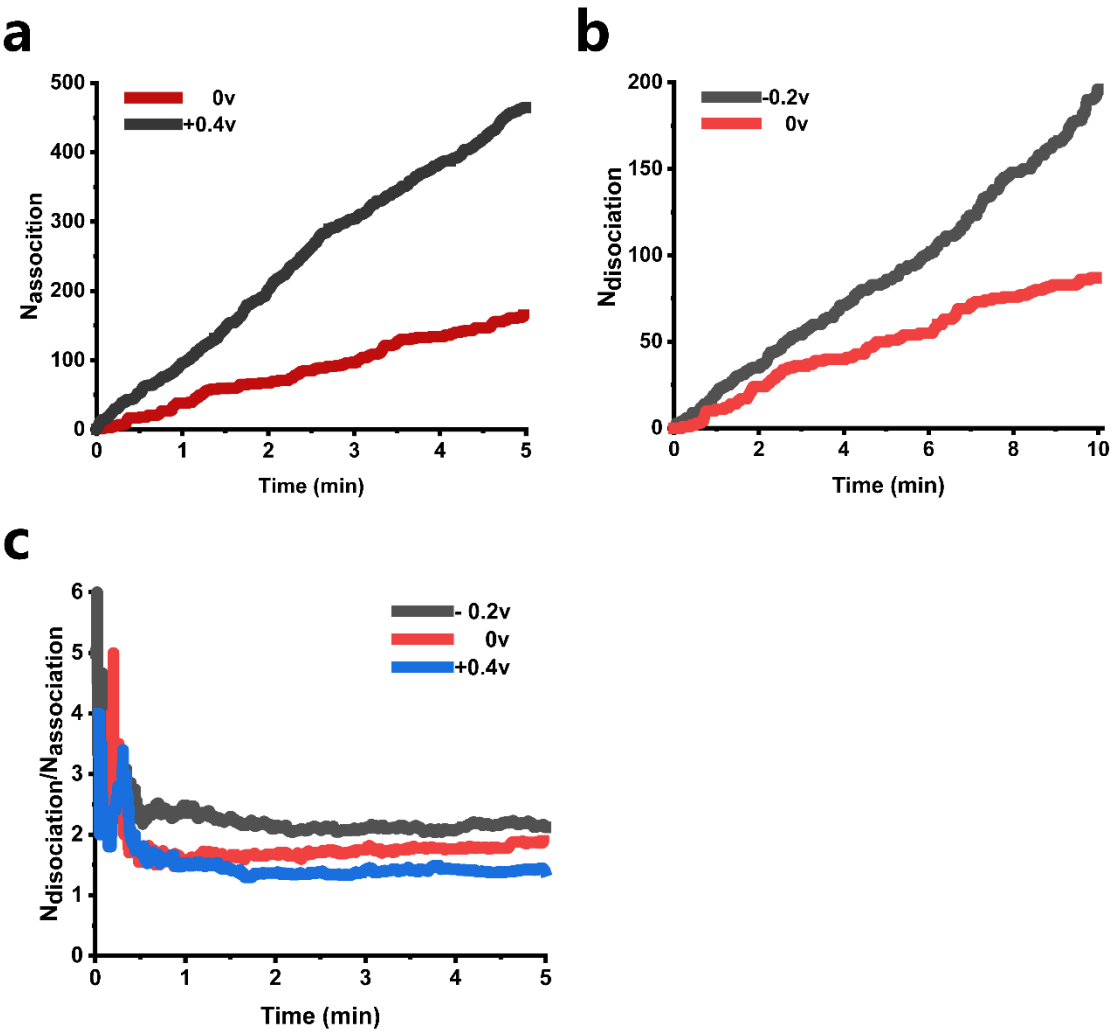

Supplementary Fig.1 Tuning molecular binding kinetics by applying electrical fields. (a) The number of binding (association) and (b) dissociation events at different applied potential (c) The ratio between binding and dissociation events. The binding events increased by nearly 3-fold (from 162 to 465) with positive potential applied, while the dissociation events were doubled with negative potential applied.

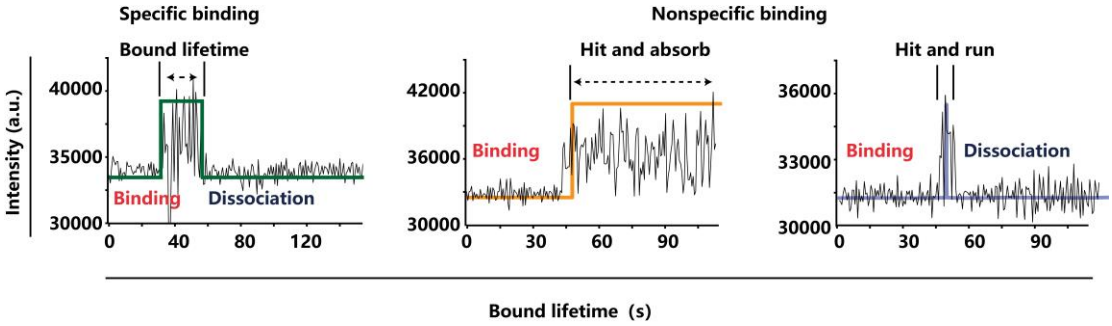

Supplementary Fig. 2 Typical intensity profile of specific binding and nonspecific binding.

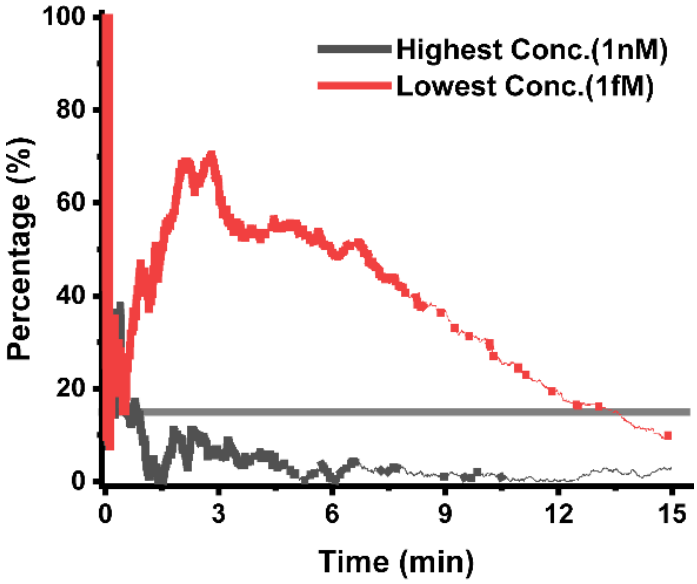

Supplementary Fig.3 Time-dependent coefficient of variation (CV) in the AuNPs association and dissociation events. The CV is calculated by standard deviations divide by the average, which scales with 1/ √ N (N is the number of events). For high concentration of analyte, the CV declined quickly at several minutes. In contrast, the CV of low analyte concentration decreased below 15% until **13.5** min. We thus determined that 15-min assay is sufficient for fM level's miRNA detection.

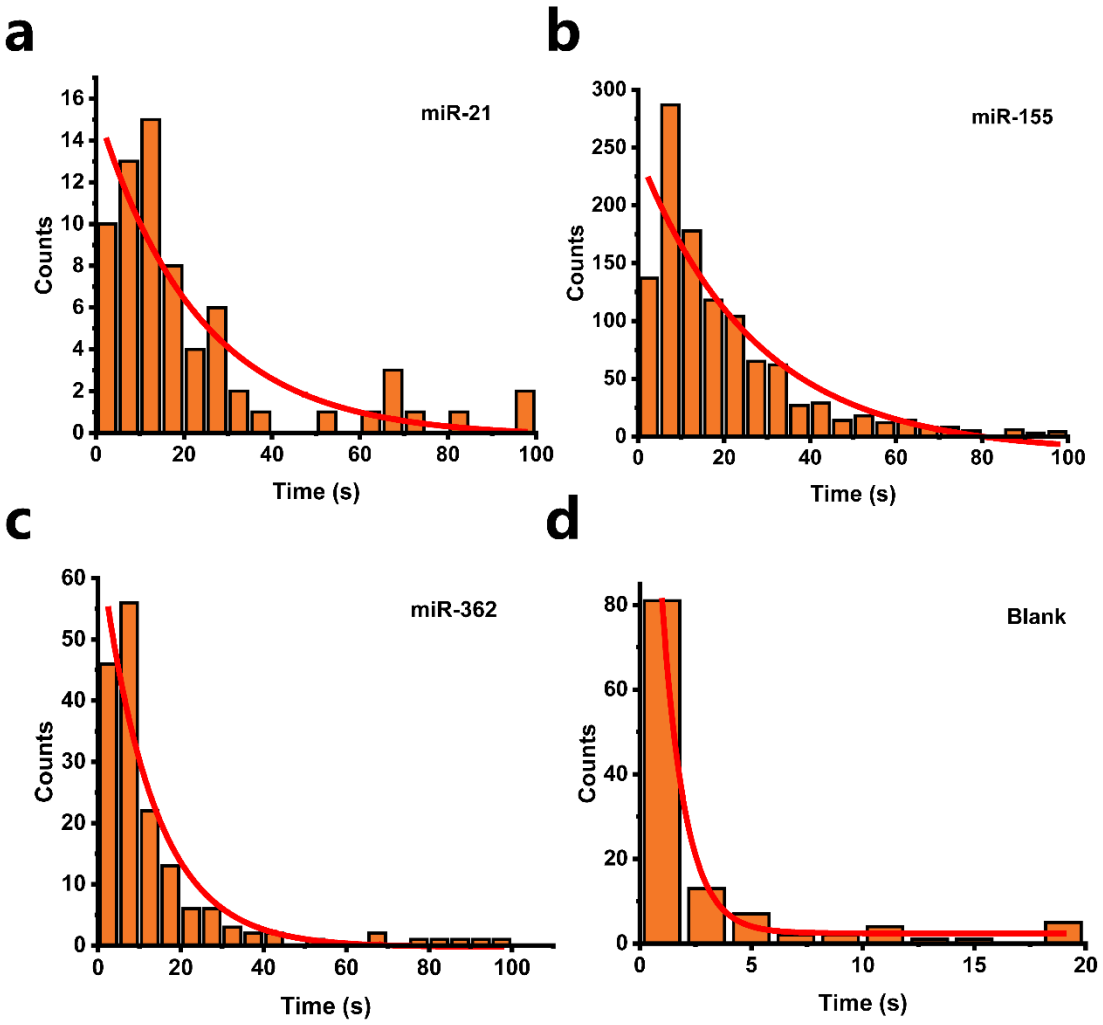

Supplementary Fig.4 Bound time distribution of three miRNA (a, b and c) and blank (d). The bound lifetime was determined via an exponential fitting. The mean ± std (n=3) values were **22.94 ± 7.49 s** for *miR-21,* **27.26 ± 8.93 s** for *miR-155*, **12.67 ± 2.35 s** for *miR-362* and **4.11 ± 0.26 s** for blank, respectively. The blank group stands for in absence of analyte.

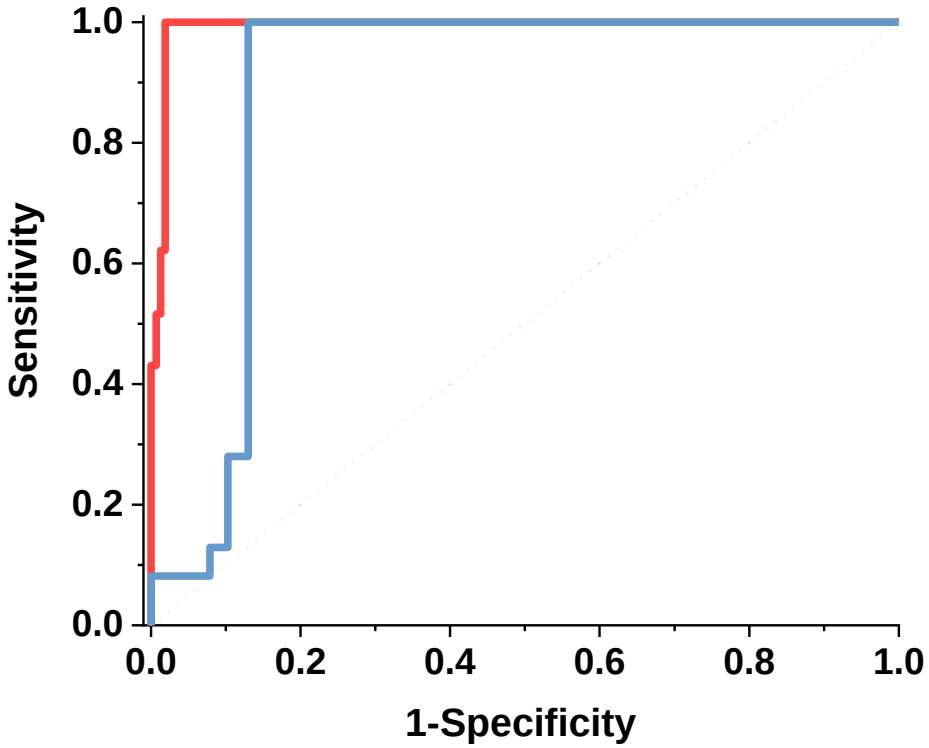

Supplementary Fig.5 The receiver operating characteristic (ROC) performance in detection of *hsa-miR-29a* with (blue) or without (red) the presence of *hsa-miR-29c*. Corresponding area under curve (AUC) is **0.979 (red), and 0.816 (blue)**. ROC curve plots were constructed by varying the bound time threshold from 0 to 20 s for discriminating between *hsa-miR-29a* and *hsa-miR-29c*.

Supplementary Note 1: Supporting Discussion

Rapid detection of nucleic acid biomarkers is important for identification of acute pathogenic infections. Typically, the clinical tests in an outpatient visit require less than 15 minutes assay time, and point-of-care testing may require even less time. Amplification-free detection of short nucleic acid targets has been achieved by digital counting of analyte molecules hybridized with probes on a sensor surface. However, highly sensitive and specific measurement has been hampered by the nonspecific surface bindings of fluorescently-labeled secondary probes. Single molecule kinetic assays such as the single-molecule recognition through equilibrium Poisson sampling (SiMREPS) circumvent this limitation by discriminating specific binding from nonspecific binding using kinetic properties. SiMREPS has demonstrated excellent sensitivity down to subfemtomolar detection limit and extremely high specificity. However, they still face two main limitations in assay time as follows.

First, the hybridization at the sensor surface represents a heterogeneous reaction, which is common for biosensors. The assay time is largely limited by the mass transportation of fluorescence-labeled DNA probes and the analyte onto the sensor surface. Thus in a typical

SiMREPS experiments, the analyte need to be incubated on the sensor surface for tens of minutes before detection. The diffusion rate in commonly used microfluidic channels could be estimated with typical values of less than 10 μm/s[1]. Considering a millimeter-order height of the channel, it takes at least minutes for the diffusion to complete, the diffusion rate was described by the Stocks-Einstein equation,

$$D_P = \frac{k_B T}{6\pi\eta r} \quad \text{(S1)},$$

Second, the hybridization kinetics are limited by the number of complementary bases between the analyte and DNA probe. It has been reported that for a longer probe, the binding rate (k_{on}) increased linearly, but the dissociation rate decreased exponentially, typically in the range of 6~9 nt[2]. However, ideally, SiMREPS requires repeated hybridization with a fast dissociation rate, but also a fast binding rate to reach equilibrium. Therefore, simply changing the length of DNA probes could not satisfy the requirement to shorten the assay time.

The SSM[3] circumvent the above limitations by the following designs. First, nanoparticles tethered to longer DNA probes are used to replace the fluorescence-labeled short DNA probes. The longer DNA probes ensure a fast binding rate to capture analyte, and the nanoparticles are manipulated to actively transport the analyte to the sensor surface. This effectively breaks the limit by mass transportation. Second, to accelerate the dissociation during detection, an external force is applied on the nanoparticle as a load on the DNA duplex. This is similar to the scheme in the single molecule force spectroscopy, which measures the lifetime of molecular bond under different loads. As a result, the SSM[3] effectively shorten the assay time to within 15 minutes in the current system.

For detection of much longer nucleic acid biomarkers, a higher number of complementary base pair of the probe would result in distinct kinetics. To adapt SSM[3] for wider applications, it's necessary to apply a much higher force on the nanoparticles. Although the present protocol makes use of AuNPs and its micromanipulation through electrical fields, it's reasonable to expect translations into other forms, such as the magnetic nanoparticles and magnetic tweezers to extend the dynamic range of detection.

Supplementary Note 2: Theoretical model

Considering the dynamics of a one-dimensional system (**Supplementary Fig.6**), the fine-tuning of binding kinetics by the nanoparticle micromanipulation could be described by the Langevin equation, [3, 4]

$$M\frac{\mathrm{d}^2 z}{dt^2} = -\frac{\mathrm{d}U(z)}{\mathrm{d}z} - 6\pi\eta a\frac{dz}{dt} + \xi(t) + F \quad \text{(S1)},$$

where M is the mass of the nanoparticle, $U(z)$ is the hybridization potential, the second term on the right is the damping due to viscosity (η is the solvent viscosity and a is the radius of the nanoparticle), ξ is the thermal fluctuation force and $F(z)$ is the applied external force. The total potential U' under external force could be written as

$$U'(z) = U(z) - \int_0^z F(Z)dZ \quad \text{(S2)}$$

The applied external force lowers the energy barrier of dissociation, and thus increases the probability that the accumulated energy from thermal fluctuation drive the system over the barrier into dissociated state. The probability ρ(t) that a molecule persists in its bound state can be approximately calculated through the kinetic equation as defined by Kramer's transition rate: [4]

$$\frac{\mathrm{d}\rho(t)}{\mathrm{d}t} = -\frac{\omega_0(t)\omega_1(t)M}{12\pi^2\eta a} e^{-\left(U_B'(t)/k_BT\right)}\rho(t) \quad \text{(S3)}$$

where U_B' is the barrier height, $\omega_0 = M^{-1}\frac{\mathrm{d}^2U'(z=0,t)}{\mathrm{d}z^2}$ and $\omega_1 = M^{-1}\left|\frac{\mathrm{d}^2U'(z=z',t)}{\mathrm{d}z^2}\right|$ are the effective oscillation frequencies at the bound state and at the maximum potential, k_B is Boltzmann constant, and T is the temperature. In the experiments, we measure the distribution of bound lifetime, which is the probability density:

$$p(\mathrm{t}) = \frac{\mathrm{d}(1-\rho(t))}{dt} = -\frac{\mathrm{d}\rho}{\mathrm{d}t} \quad \text{(S4)}$$

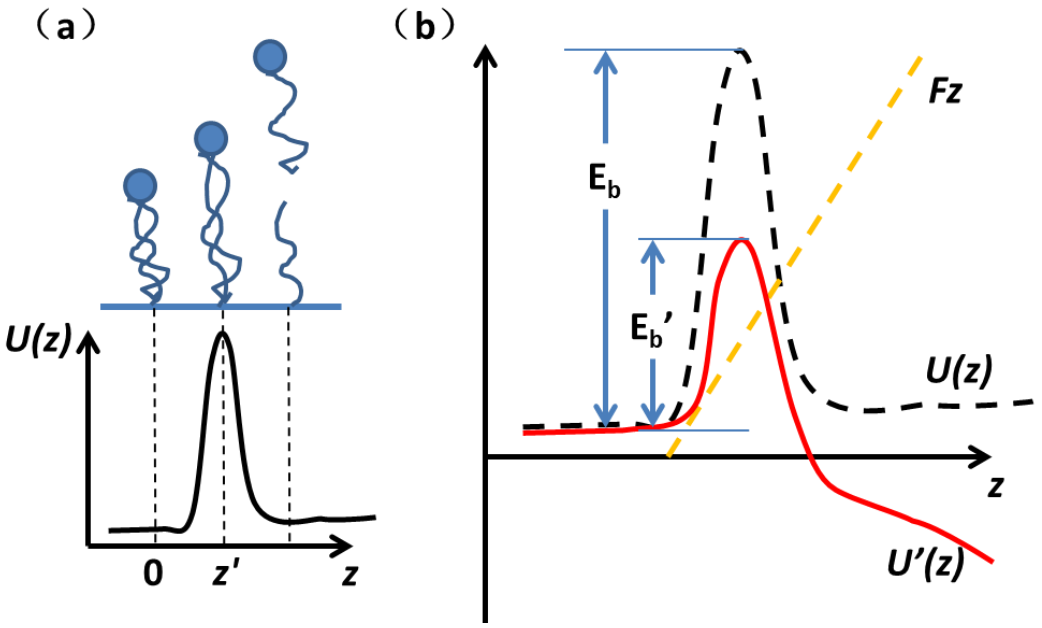

Supplementary Fig.6 The theoretical model in SSM[3]. (a) The one-dimensional model system and the adhesion potential. (b) The adhesion potential under external force manipulation.

Supplementary Note 3: Binding kinetics under different voltages

Consistent with our expectation, in **Fig. 1c**, the bound lifetime decreased from 43.8 s at +0.4 V to 30.2 s at -0.4 V, corresponding to an increased dissociation rate. The number of total binding and dissociation events shows a more complicated trend. Compared with the control without

applying voltage (at 0V), the increased number of events at +0.2 V is due to the active transportation of nanoparticles to sensor surface, beating the passive diffusion limit. At +0.4 V, although stronger active mass transportation led to more binding events, the dramatic increase of the bound lifetime hampered the repeated binding, resulting in a net decrease of events. At -0.2 V, the observed binding and dissociation events increased by 3-fold due to the enhanced repeated binding, as the bound lifetime decreased dramatically. At -0.4 V, while the bound time did not change much, the strong pulse force prevent the nanoparticles from approaching the sensor surface, and resulted in less total events observed.

Supplementary Note 4: ROC plot, and discrimination factor Q calculation

The specificity of an assay is calculated from the number of true negatives (TN) and false positives (FP) according to the relationship:

$$specificity = \frac{TN}{TN+FP} \quad \text{(S5)}$$

In which, TN is true negative, FP is false positive.

The discrimination factor Q was calculated as:

$$Q = \frac{Events\ of\ target\ analyte}{Events\ \ of\ undesired\ molecule} \quad \text{(S6)}$$

Supplementary Note 5: miRNA synthesis and probe design.

For experimens in tuning the binding kinetics with electrical force (**Fig.1c**), we synthesis the 50-nt oligo-analyte and 25-nt DNA probes in **Table S1**. Note that the underlined sequences of target nucleic acid and capture probe were complementary, and the blue-marked sequences of target nucleic acid and detection probe were complementary.

Supplementary Table 1. Synthesized oligo-analyte and DNA probes for experiments in tuning the binding kinetics

Name		Sequence		length
Oligo-analyte	5’	GCGTAAAAGAGAAGCTGATCGAGAA AGCAGGCGCGTGGTACAGCTACAAA	3’	50 nt
Capture probe	3’	HS- CGCATTTTCTCTTCGACTAGCTCTT	5’	25 nt
Detection probe	3’	AGCAGGCGCGTGGATGTCGATGTTT –biotin	5’	25 nt

For miRNA detection experiments, the corresponding sequences were shown in **Table S2.** Note that the red-marked capture probe sequences represent lock nucleic acid (LNA) rather than DNA nucleotides, which provide much higher affinity to the target analyte. The capture probe was thiol-functionalized at 3’ and both detection probes were biotin-functionalized at 5’.

Supplementary Table 2. The miRNAs and corresponding capture probes and detection probes.

Name		Sequence		length
miR-21	5′	UAGCUUAUCA GACUGAUGUUGA	3′	22 nt
Capture probe	3′	HS- ATCGAATAGT	5′	10 nt
Detection probe	3′	CTGACTACAACT -biotin	5′	12 nt
miR-155	5′	UUAAUGCUAAU CGUGAUAGGGGU	3′	23 nt
Capture probe	3′	HS- AATTACGATTA	5′	11 nt
Detection probe	3′	GCACTAT CCCCA -biotin	5′	12 nt
miR-362	5′	AAUCCUUGGAAC CUAGGUGUGAGU	3′	24 nt
Capture probe	3′	HS-TTAGGAACCTTG	5′	12 nt
Detection probe	3′	GATCCACACTCA -biotin	5′	12 nt

For single base pair mismatch experiments, the sequences are listed in the **Table S3**. The detection probe was designed to be complementary to *miR-29a* but with one base pair mismatch to *miR-29c*.

Supplementary Table 3. The miRNAs and oligonucleotides probes for single base pair mismatch experiments.

Name		Sequence		length
miR-29a	5′	UAGCACCAUCUG AAAUCGGUUA	3′	22 nt
miR-29c	5′	UAGCACCAUUUG AAAUCGGUUA	3′	22 nt
Detection probe	3′	biotin- ATCGTGGTAGAC	5′	12 nt
Capture probe	3′	TTTAGCCAAT -SH	5′	10 nt

REFERENCES

1. Squires, T.M., Messinger, R.J. & Manalis, S.R. *Nat Biotechnol* **26**, 417-426 (2008).
2. Dupuis, N.F., Holmstrom, E.D. & Nesbitt, D.J. *Biophys J* **105**, 756-766 (2013).
3. Hänggi, P., Talkner, P. & Borkovec, M. *Reviews of modern physics* **62**, 251 (1990).
4. Dudko, O.K., Filippov, A.E., Klafter, J. & Urbakh, M. *Proc. Natl. Acad. Sci. USA* **100**, 11378-11381 (2003).